STUDY ON PHOTOCATALYSIS PROPERTY OF Er^{3+} DOPED Bi_2MoO_6 BY HYDRO-THERMAL METHOD

S. CHANG, F. LI, Y. CAI, Y. SHEN[*]
Hebei Provincial Key Laboratory of Inorganic Nonmetallic Materials, College of Materials Science and Engineering, North China University of Science and Technology, Tangshan, Hebei, 063210, P. R. China

In this study, Bi_2MoO_6 with different Er^{3+} doping amount was successfully synthesized via hydro-thermal method. The influence of Er^{3+} concentration on photocatalysis property was investigated. The phase structures were analyzed by X-ray diffraction. The microstructures were measured by scanning electron microscopy. The photocatalysis property was measured by the degradation of Rhodamine B. The results showed that Bi_2MoO_6: Er^{3+} achieved the best photocatalysis property when the Er^{3+} concentration was 0.05% and the degradation ratio reached 93.30% after 180min illumination. Raman spectra, UV-vis. DRS and the dynamics of RhB photodegradation reaction for the samples of Bi_2MoO_6 when the Er^{3+} concentration was 0.00% (B) and 0.05% (E/B) confirmed the improvement mechanism of photocatalytic performance. The peaks in Raman spectra were found at 140 cm^{-1}, 197 cm^{-1}, 284 cm^{-1}, 323 cm^{-1}, 351 cm^{-1}, 716 cm^{-1}, 799 cm^{-1}, 842 cm^{-1}. UV-vis. DRS spectra of B and E/B suggested 0.05% doping of Er^{3+} increased the absorbtion range of visible light. The dynamics of RhB photodegradation reaction ($-\ln(C/C_0)$) for the samples of B and E/B showed that the reaction ratio of B was 0.00361 min^{-1} and E/B was 0.01193 min^{-1}. E/B achieved a better photocatalysis property than B.

1. Introduction

Nowadays, environmental pollution problems and energy problem are becoming more and more serious with the development of industry, which need to be solved severely, especially in China[1]. Photocatalytic materials such as TiO_2[2]、ZnO[3]、Ag_3PO_4[4]、SnS_2[5]、$BiVO_4$[6]、$BiFeO_3$[7] have been studied for a long time. And TiO_2 pholocatalyst was the most studied. However, this oxide can be activated only by UV irradiation, which limited its range of application. The energy band gaps of Bi_2MoO_6 samples were found to be about 2.60eV. So it can improve the photocatalytic activity in the visible range. Bi_2MoO_6:Er^{3+} as a new semiconductor pholocatalyst is expected to offer promising applications in the field of wastewater treatment[8] and degradation of organic pollutants. Bi_2MoO_6:Er^{3+} as a promising material is worth being invested. Various techniques such as ion doping strategy[9]、acquiring composite materials and using additives[10] have been used to enhance the photocatalytic activity of Bi_2MoO_6:Er^{3+}. In the past years, in order to achieve the photocatalytic mechanism of Bi_2MoO_6:Er^{3+}, it was prepared by sol-gel method[11]、soft-chemical [12]、 hydrothermal method[13]. The hydrothermal technique is an economical and easy way for the morphology and local structure to control of such material[12].

---

[*] Corresponding author: tlteba@163.com

In this study, pure orthorhombic Bi_2MoO_6 were synthesized via hydro-thermal method. Photocatalytic activity of $Bi_2MoO_6:Er^{3+}$ has been investigated by controlling the Er^{3+} doping amount form 0%~5%. The photocatalytic performance has been discussed through degradating the RhB, Raman spectra, UV-vis and the dynamics of RhB photodegradation reaction for the samples of Bi_2MoO_6 when the Er^{3+} concentration was 0% (B) and 0.05% (E/B).

2. Experimental

2.1. Preparation of $Bi_2MoO_6:Er^{3+}$ with different Er^{3+} doping amount

All reagents used in our experiment were of analytical purity and used without further purification. The raw materials $NaOH$, HNO_3, Na_2MoO_4, $Bi(NO_3)_3\cdot5H_2O$, Er_2O_3 were employed in this experiment. $0.001mol$ Na_2MoO_4 and $0.002mol$ $Bi(NO_3)_3\cdot5H_2O$ were dissolved in 10ml 3.6mol/L HNO_3 solution followed by addition of Er_2O_3 which should be weighed accurately controlling the molar ratio of Er^{3+} and Bi^{3+} of 0.01%, 0.05%, 0.1%, 0.5%, 1%, 3%, 5%. The pH value was adjusted to 6 by slowly adding 2mol/L $NaOH$ solution. The resulting solution was then transferred into the Teflon-lined autoclaves, and was heated to 160℃ for 12h. The precipitation was alternately washed by distilled water and anhydrous ethanol three times. The final production was achieved after drying and grinding.

2.2. Characterization

The X-ray diffraction (XRD) patterns were recorded using an X-ray diffractometer (Rigaku D/Max-2500) with Cu Kα radiation (λ =0.15406 nm)，and diffraction angles ranging from 10° to 90°. The sample's microstructures were analyzed by scanning electron microscopy (SEM, Hitachi Limited, Japan). The photocatalysis property was investigated by recording the ratio of decomposing 5mg/L rhodamine B after 180min illumination, Raman spectra, UV-vis. DRS and the dynamics of RhB photodegradation reaction for the samples of Bi_2MoO_6 when the Er^{3+} concentration was 0.00% (B) and 0.05% (E/B).

3. Results and discussions

Fig. 1 shows the XRD patterns of Bi_2MoO_6 prepared with different Er^{3+} doping amount form 0%~5%. And those diffraction peaks were attributed to the orthorhombic Bi_2MoO_6 phase when the Er^{3+} doping amount was 0.01%, 0.05%, 0.1%, 0.5%, 1%, 3%, 5%. While the Er^{3+} doping amount was 0%, Cubic Bi_2O_3 phase was appeared with orthorhombic Bi_2MoO_6 phase. This suggested that the existence of Er^{3+} made the crystal phase of $Bi_2MoO_6:Er^{3+}$ pure, reducing the generation of other component.
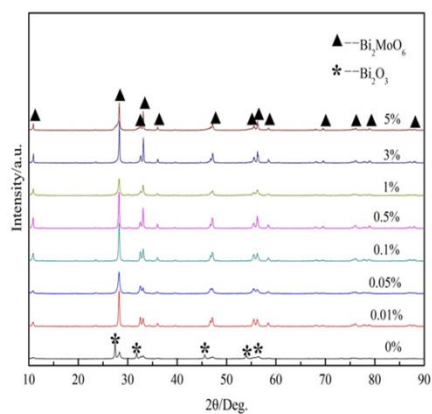
Fig. 1 XRD patterns of Bi$_2$MoO$_6$ catalysts doped with different Er^{3+} ratios
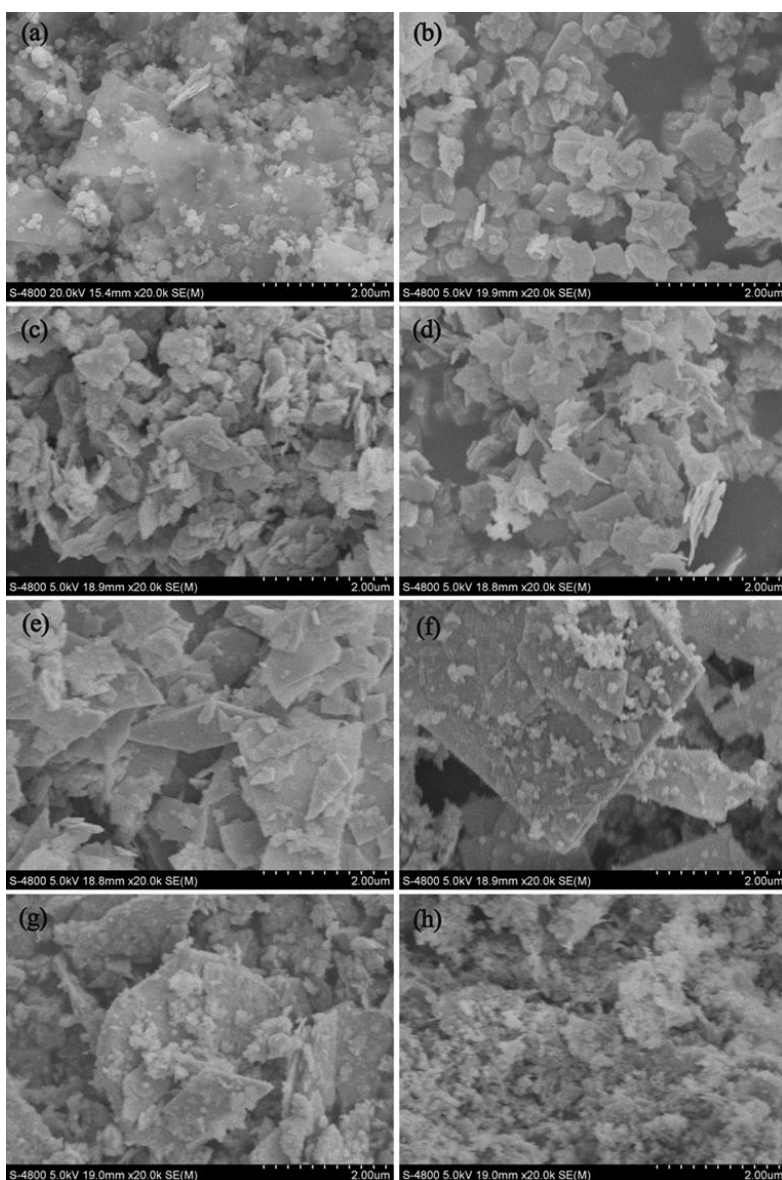
Fig. 2 SEM picture of Bi$_2$MoO$_6$ catalysts doped with different Er^{3+} ratios

Fig. 2 shows the SEM images of the Bi_2MoO_6 samples prepared hydrothermally when the Er^{3+} doping amount was 0%, 0.01%, 0.05%, 0.1%, 0.5%, 1%, 3%, 5%. From the above SEM images, it was observed that the Bi_2MoO_6 sample was nanosheet structure and some nanosphere structure when the Er^{3+} doping amount were 0.01%, 0.05%, 0.1%, 0.5%, 1%. With the increasing of Er^{3+}, nanosheet structure got more and more large and thick. Maybe Er^{3+} can promote the growth of crystal phase. Continuing to increase Er^{3+}, Crystal phase agglomerated seriously with the Er^{3+} doping amount of 3%. The surface of Bi_2MoO_6 crystal phase had been destroyed badly when the Er^{3+} doping amount was 5%. The contents of excessive Er^{3+} will lead to the lattice distortion of Bi_2MoO_6. When the doping amount of Er^{3+} was 0.05%, Bi_2MoO_6: Er^{3+} was nanosheet shape of neat edge and dispersed evenly. It can be indicated that there is a crucial influence on the morphology of the Er^{3+} concentration.
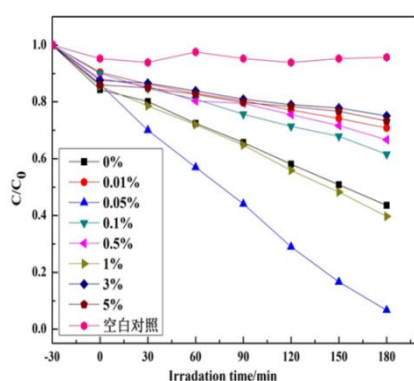
Fig. 3 degradation chart of Bi_2MoO_6 catalysts doped with different Er^{3+} ratios

Fig. 3 displayed the photocatalytic activities of the Bi_2MoO_6:Er^{3+} samples in the degradation for 180min. The blank test affirms that the degradation of Rhodamine B is very slow if no photocatalyst was added. As shown in Fig. 3, Orthorhombic Bi_2MoO_6: Er^{3+} achieved the best photocatalysis property when the Er^{3+} doping amount was 0.05%. Its degradation ratio reached 93.30% after 180min illumination. The degradation ratio of the blank test was 56.39% at the same condition. The worst photocatalytic activity was shown when added 3% of Er^{3+} and its degradation ratio only achieved 24.94% after 180min illumination. Only a suitable proportion of uranium ion doping can greatly enhance the photocatalytic performance of bismuth molybdate samples.
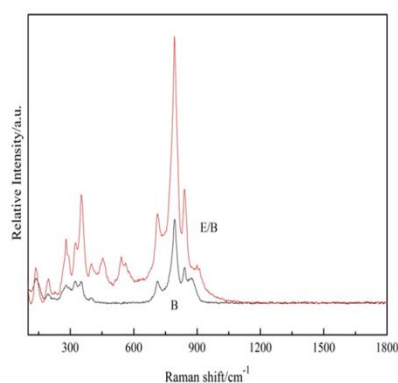
Fig. 4 Raman spectra of B (0% of Er^{3+}) and E/B (0.05% of Er^{3+})

Raman spectra of B and E/B confirmed the XRD result in Fig. 4. The peaks in Raman spectra at 140 cm^{-1}, 197 cm^{-1}, 284 cm^{-1}, 323 cm^{-1}, 351 cm^{-1}, 716 cm^{-1}, 799 cm^{-1}, 842 cm^{-1} indicated

that the phase of B and E/B was Bi_2MoO_6. E/B samples have three more peaks which were found at 400 cm^{-1}, 453 cm^{-1}, 541 cm^{-1} than B samples. The relative intensity of E/B was higher than B. Maybe the presence of Bi_2O_3 reduced the purity of the crystalline phase.
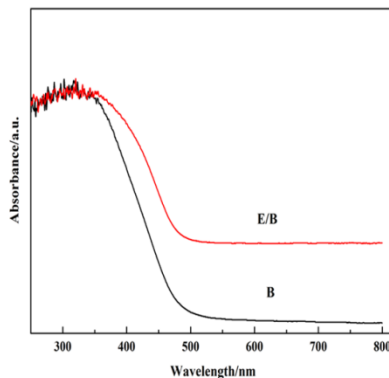
Fig. 5 UV-vis. DRS spectra of B (0% of Er3+) and E/B (0.05% of Er3+)

As is shown in Fig. 5, the absorption edge of B was about 500nm, and E/B's absorption edge relative redshift. The band gap of E/B becomes narrower. It proved that E/B can absorb visible light with a wavelength larger than B. This was the reason why the photocatalytic performance was improved.
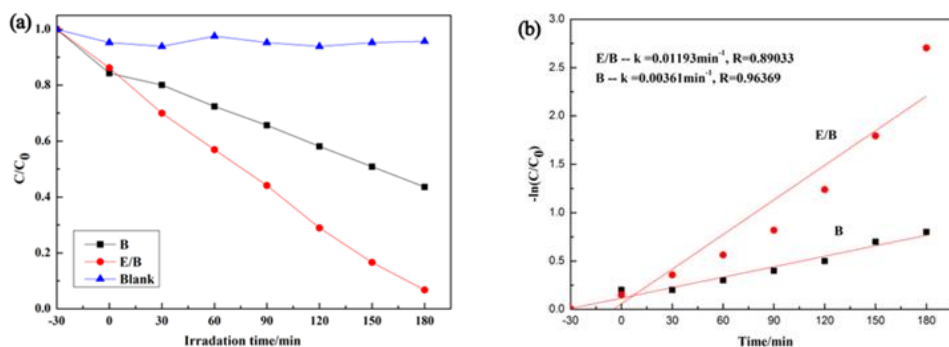
Fig. 6 RhB degradation of B (0% of Er^{3+}) and E/B (0.05% of Er^{3+}) (a) and the dynamics of RhB photodegradation reaction (-ln(C/C_0) versus time) for the B (0% of Er^{3+}) and E/B (0.05% of Er^{3+}) (b)

The RhB degradation of the samples (a) and the dynamics of RhB photodegradation reaction (-ln(C/C_0) versus time) for the samples (b) were represented in Fig. 6. From the Fig. 6(a), the degradation ratio of B was 56.39% and E/B was 93.30%. Fig. 6(b) showed the relationship between -ln(C/C_0) and reaction time. The reaction rate constant of E/B (k=0.01193min^{-1}) was greater than B (k=0.00361min^{-1}). This demonstrated that E/B had superior photocatalytic properties.

4. Conclusions

Bi$_2$MoO$_6$:Er^{3+} were successfully fabricated by controlling the Er^{3+} doping amount during the reaction process via hydro-thermal method. The XRD, SEM and Raman spectra results suggested that crystal phase and morphology are connected with the Er^{3+} doping amount. Photodegradation rate of RhB indicated that Bi$_2$MoO$_6$:Er^{3+} synthesized when the Er^{3+} doping was 0.05% achieved the best photocatalysis property. UV-vis. DRS and the dynamics of RhB photodegradation reaction for the samples of Bi$_2$MoO$_6$ when the Er^{3+} concentration was 0.00% (B) and 0.05% (E/B) demonstrated that the redshift of absorption edge and higher reaction rate constant were good for the promotion of photocatalytic activity.

Acknowledgements

References

[1] X. L Tian, Q. G Guo, C Han, N Ahmad, Global Environmental Change. **39**, 244 (2016).

[2] Q Wang, J Lian, Y Bai, J Hui, J Zhong, J Li, et al. Materials Science in Semiconductor Processing. **40**, 418 (2015).

[3] S. K Shahi, N Kaur, J. S Shahi, V Singh. Investigation of morphologies, photoluminescence and photocatalytic properties of ZnO nanostructures fabricated using different basic ionic liquids[J]. Journal of Environmental Chemical Engineering. (2016).

[4] K Baďurová, O Monfort, L Satrapinskyy, E Dworniczek, G Gościniak, G Plesch. Ceramics International. **43**(4), 3706 (2017).

[5] J. H Liu, G. F Huang, W. Q Huang, H Miao, B. X Zhou, Materials Letters. **161**, 480 (2015).

[6] O Monfort, S Sfaelou, L Satrapinskyy, T Plecenik, T Roch, G Plesch, Catalysis Today. **280**, 51 (2017).

[7] Y. Guo, Y. Pu, Y. Cui, C. Hui, J. Wan, C. Cui. Materials Letters. **196**, 57 (2017).

[8] X. Wang, P. Tian, Y. Lin, L. Li, Journal of Alloys and Compounds. **620**, 228 (2015).

[9] Y Zhang, Y Ma, Q Liu, H Jiang, Q Wang, D. Qu, Ceramics International. **43**(2), 2598 (2017).

[10] R. J Carmona, L. F Velasco, M. C Hidalgo, J. A Navío, C. O Ania, Applied Catalysis A: General. **505**, 467 (2015).

[11] V. Umapathy, A. Manikandan, S. A. Antony, Transactions of Nonferrous Metals Society of China, **25**(10), 3271 (2015).

[12] X. Ding, W. Ho, J Shang, et al. Applied Catalysis B Environmental **182**, 316 (2016).

[13] A. Phuruangrat, P. Dumrongrojthanath, S. Thongtem, et al. Materials Lettrs **194**, 114 (2017).